Precision Engineering 35 (2011) 143–152

Contents lists available at ScienceDirect

Precision Engineering

journal homepage: www.elsevier.com/locate/precision

Fuzzy-logic control of cutting forces in CNC milling processes using motor currents as indirect force sensors

Dohyun Kim*, Doyoung Jeon

Department of Mechanical Engineering, Sogang University, 1 Sinsu-dong, Mapo-gu, Seoul 121-742, Republic of Korea

ARTICLE INFO

Article history:
Received 25 May 2010
Received in revised form 18 August 2010
Accepted 1 September 2010
Available online 15 September 2010

Keywords:
Fuzzy-logic control
Force control
CNC machining center
Milling process
Spindle motor current
Force sensor

ABSTRACT

A fuzzy-logic controller (FLC) is designed to automatically adjust feed rate in order to regulate the cutting force of milling processes in a vertical machining center. The FLC has a double-loop structure, consisting of the inner PD (proportional-derivative) velocity-control loop for a feed servo and the outer fuzzy-logic force-control loop. Reference cutting forces are well maintained in both numerical simulation and experiments when the cutting-depth profile of an aluminum workpiece (Al6061-T6) is varying step-wise or continuously. In order to replace expensive and impractical tool dynamometers, ac-induction-motor currents in the feed system and the spindle system are analyzed, and then compared as a cutting-force sensor. The bandwidth of both systems are not high enough to sense the cutting dynamics for common spindle speeds. Thus, quasi-static quantities (i.e., average or maximum resultant cutting force per spindle revolution) are compared instead. The spindle-motor current is chosen because quasi-static sensitivity is much higher (i.e., 5.415×10^{-3} vs. 2.128×10^{-4} A/N). Reference cutting forces (230 and 330 N) are well maintained when the depth of cut is less than 4 mm.

1. Introduction

Process control of CNC-aided machine tools is used to maximize productivity while maintaining part quality and integrity of machine tools [1]. However, process controls such as control of chatter, cutting force, and tool condition, have not been fully integrated into commercial machine tools even after decades of research and development [2]. The difficulties include a lack of affordable and accurate process-monitoring tools, and robust control algorithms that can cope with complex, nonlinear, time-varying and sometimes unpredictable machining processes.

In machining, a high metal-removal rate (MRR) is an important factor that determines productivity. However, the cutting parameters (i.e., spindle speed and feed rate) are usually set at a constant value in a conservative manner. Or a skilled technician constantly monitors machining processes and modifies cutting parameters to prevent excessive machining forces from causing machine-tool damage. As a result, it is difficult to maximize productivity when effective process monitoring and control are not available.

Automation of machining processes using ACC (adaptive control with constraint), in which the machining parameters are adjusted in real time to have adequate process variables, has been studied [2]. Maintaining machining forces at a maximum allowable level by automatically controlling cutting parameters results in improvement of productivity [3]. Model-based control algorithms have been studied extensively. Fixed-gain control was not effective [4] due to dynamically varying model parameters which depend on cutting parameters [1]. Thus, adaptive control was introduced to account for changes in the model parameters over time [4–8]. Control algorithms robust to a range of parameters or model variations were also studied recently [9–12]. However, all of these approaches have not lived up to industry expectations, mainly because of the lack of accurate models for complex and nonlinear machining dynamics, and tremendous inherent variation of force processes [13].

Fuzzy-logic control, an artificial-intelligence-based method, is a viable alternative to model-based control schemes. Skilled human operators are shown to be better than model-based controllers in machining control [14]. The human experience can cope with uncertainty and complexity of machining process successfully [15]. Human operators express the process variables in "imprecise" language (i.e., linguistic variables) and apply them to the control of machine tools. A lack of accurate models, model parameters, and exact numerical values of machining conditions is not a problem. Thus, human-based methods of obtaining control outputs (i.e., cutting parameters) can be adapted to the constant-force control that maximizes MRR. Fixed-rule fuzzy controllers [15,16] and

* Corresponding author. Present address: Bioengineering Department, University of California, Berkeley, 342 Stanley Hall, Berkeley, CA 94720, United States. Tel.: +1 510 647 4353; fax: +1 510 642 5835.
E-mail address: dohyun@berkeley.edu (D. Kim).

0141-6359/$ – see front matter © 2010 Elsevier Inc. All rights reserved.
doi:10.1016/j.precisioneng.2010.09.001

learning-capable fuzzy schemes [17,18] have been studied, and implemented on milling processes.

The cutting forces of a milling process are usually measured with a table-mounted tool dynamometer in research laboratories. A dynamometer is expensive, axis travels are limited, and cutting fluid can damage the dynamometer [19]. As a result, dynamometers are not widely used in the industry. Thus, much effort has been devoted to developing indirect force-measurement tools.

Various mechanical or electrical variables of feed- and spindle-system conditions have been studied to estimate forces. For spindle systems, Shuaib et al. [20] installed a strain gauge between the spindle axis and the tool, and then measured cutting torque. It is advantageous to measure the cutting force at a spindle because it is close to the cutting point. However, complexity of spindle integration is problematic. The space for installation is limited in many spindle systems without significant modification [21]. Wiring of the sensor installed at the rotating spindle is not simple. Shuaib et al. used a garter-spring pickup for signal transmission. Electrical noise and abrasion due to the constant contact render this approach unreliable. More modern torque measurement based on piezo-quartz transducers (i.e., rotating dynamometer) transmits signal wirelessly, but this device is also very expensive, requires special tooling, makes it difficult to use tool changer, and changes process dynamics. Bertok et al. [22] predicted a spindle-motor torque using an empirical equation of MRR and workpiece-tool contact area. The spindle current, that was calibrated with a dynamometer, was used to identify parameters of the equation. The average cutting torque was predicted off-line using the equation, solid models of workpiece material and tool, and NC data for tool path. This approach may provide a rough guide for parameter settings prior to actual machining, and can be used as a tool condition monitoring if the measured torque is far off the predicted value. It may not be appropriate as an alternative sensor for real-time cutting-force control because there is no mechanism to compensate an unavoidable discrepancy between the predicted and measured torque (e.g., tool wear, inaccurate solid model, axis misalignment, workpiece flatness error). Also, using maximum torque information is better than using average torque of their work in preventing machine-tool damage.

Current and power of motors in a machine tool have been studied as an alternative sensor. As current and power are variables describing electromechanical systems (i.e., feed and spindle axes), the system dynamics must be identified prior to the use of sensor. These electromechanical systems act as a low-pass filter, so that the bandwidth of sensor is low compared to a dynamometer. The power consumed by cutting processes is usually a small portion of the total power that a feed or spindle system requires, so they are generally less accurate [21]. Nevertheless, current and power are attractive for industrial applications. These methods are possibly the most easily accessible variables. Additionally, current and power sensors are very cheap compared to dynamometers. It is easy to install sensors with simple retrofitting, and even some motor drives have built-in current readings. Current and power measurement does not obstruct machining processes. Stein and Wang [23] used a current sensor (i.e., hall-effect current transducer) and voltage transformer to obtain spindle-power consumption in a milling machine. Then the cutting torque was estimated using the rotor input power and synchronous speed measured with an optical shaft encoder. For feed systems, Altintas [24] measured the dc-motor currents of feed drives in a vertical milling machine. Stein et al. [25] characterized the dc-motor current of the feed system in a CNC lathe. Lee et al. [26] used the ac-motor currents to predict the cutting forces in an NC milling machine. Mannan and Broms [27] also used a setup similar to Stein and Wang. They used the spindle power to calculate cutting torque, and feed motor currents to obtain feed force in turning, milling, and drilling operations. For all these cases, the correlation between current/power and cutting force/torque are preidentified using a dynamometer.

In this study, currents of an ac-induction motor for both the feed and spindle systems are compared in terms of sensitivity and bandwidth to assess their applicability to fuzzy-logic-based cutting-force control of a milling process. To our knowledge, there has been no attempt to compare both the currents as an alternative force sensor for this purpose. After the comparison, the spindle motor current is selected due to its superior performance. The design procedure of the cutting-force controller is as follows: (1) A mathematical description of cutting forces in x and y axes was derived, and verified using actual cutting-force data measured with a dynamometer (2) A servo controller for y-axis feed and the FLC for cutting-force regulation are designed. (3) The numerical simulation based on the cutting-force model, and machining experiments are performed to verify whether the FLC successfully maintains a constant force by adjusting the feed rate in real time for varying depth of cut. (4) Motor currents of feed and spindle systems are characterized in terms of sensitivity and bandwidth using a mathematical model and cutting-force data. (5) The cutting force is estimated using the spindle-motor RMS (root-mean square) current, and using the predetermined relationship between the current and cutting force measured with a tool dynamometer. Milling experiments with varying depth of cut are performed to verify the proposed force-control system.

2. Experimental apparatus

2.1. Machine tool

A vertical machining center, ACE-V30 (Daewoo Heavy Industries, Incheon, South Korea), equipped with a built-in controller (System 100M, Korea Industrial Electronics Co., Ltd., Seoul, South Korea) was used in this work. Two-flute flat-end mills (YG-1 Co. Ltd., Incheon, South Korea) were used for cutting experiments. Diameters of the end mills were 8, 10, and 12 mm.

2.2. Workpiece material

Workpiece material was Al6061-T6 aluminum. Aluminum blocks were machined to have multiple steps of depth of cut or a linearly varying depth of cut using the built-in controller and simple G codes.

2.3. Dynamometer

A tool dynamometer (Model 9257B, Kistler Instrumente AG, Winterthur, Switzerland) was mounted on the table of the ACE-V30. The dynamometer has multiple quartz-based piezoelectric force transducers in a steel housing. When force is acting on the dynamometer, each transducer produces a charge proportional to the force component sensitive to that axis. The 9257B model measures force in x, y, and z axes (no torque measurement). The charge is then converted into voltage signal using a multi-channel charge amplifier (Model 5019A, Kistler). The measuring range is ± 5 kN. Sensitivity is -7.5 pC/N for x and y axes and -3.7 pC/N for z axis. Force data in voltage signal are sampled at 1 kHz with a DAQ (data acquisition) board (Model DS2201, DSPACE Inc., Wixom, MI, USA).

2.4. Current sensor

A 9-channel current-sensor board made in-house, was installed in the electrical cabinet to measure motor currents of feed and spindle systems. Hall-effect current transducers (LX-10, Nana Electronics, Tokyo, Japan) on the board convert 3-phase current outputs

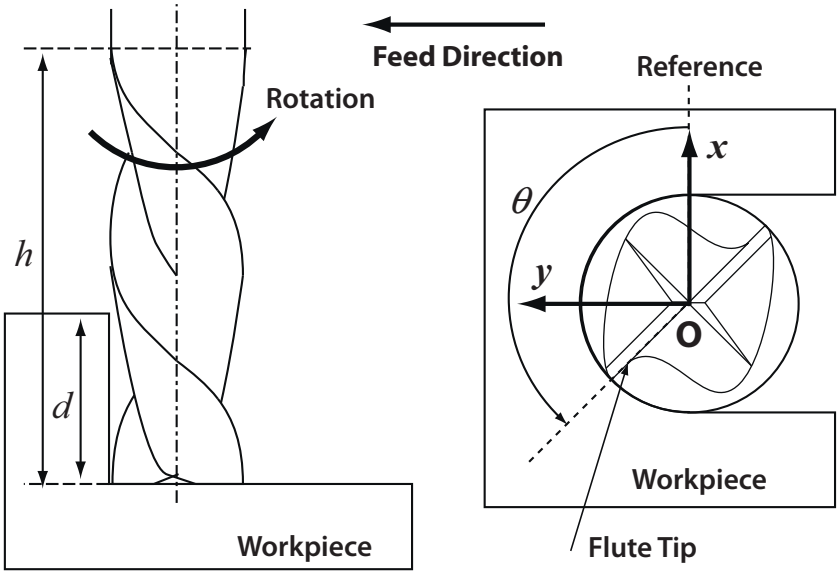

Fig. 1. Geometry of a two-flute end-milling cutter and workpiece in full immersion.

(i.e., U, V, W) of a motor drive into voltage signals, which are collected using the DAQ system.

2.5. Control system

When implementing the FLC for cutting-force regulation, a motion-control DSP (digital signal processing) system (Model DS1003), encoder board (Model DS3001), and the Model DS2201 DAQ board were used (all made by DSPACE). The control algorithm was written in C language. A PC software package (Cockpit and Trace, DSPACE) was used to monitor machine-tool conditions and change machining parameters. Numerical simulations were written and run in Matlab (The MathWorks, Inc., Natick, MA, USA).

3. Cutting-force model of end-milling processes

A mathematical model is used to predict dynamic cutting forces as a function of machining conditions in two-flute end-milling process. Milling is a complex dynamic process (e.g., non-linear, time variant). Furthermore, various vibrations that occur during cutting can cause variation in cutting forces [28]. Derivation of a rigorous mathematical model is beyond the scope of this study. Therefore, the mathematical description of cutting forces that Zheng et al. proposed [29] was adapted to use in numerical simulation later. It was assumed that cutter was perfectly aligned with respect to its spindle axis. Also, tool, dynamometer, and workpiece were assumed to be rigid in this model. Only a full immersion case (the difference between the entry angle and exit angle of a flute is 180°) was considered in this work as shown in Fig. 1. Cutting forces in x and y axes are described as:

$$F_x = \frac{K_s K_{rt} f_t d}{2} + \frac{K_s f_t h}{4\pi} \sin\left(\frac{2\pi d}{h}\right) \sqrt{1+K_{rt}^2} \sin\left(2\theta - \frac{2\pi d}{h} + \psi\right),$$

$$\text{and} \quad F_y = \frac{K_s f_t d}{2} - \frac{K_s f_t h}{4\pi} \sin\left(\frac{2\pi d}{h}\right) \sqrt{1+K_{rt}^2} \sin\left(2\theta - \frac{2\pi d}{h} + \psi\right). \tag{1}$$

In this expression, K_s is the tangential specific cutting force, and $\tan\psi = 1/K_{rt}$ where K_{rt} is the radial-to-tangential cutting-force ratio [30]. The distance that the center of the tool **O** travels is $f_t = f/(N_s \cdot M)$, where f is the feed rate (mpm), N_s is the spindle speed (rpm), and M is the number of flutes. θ is the rotational angle of the flute tip, and h is the length of cut. The cutting forces are functions of time t, because $\theta = 2\pi N_s t/60$. It was assumed that only a single flute engages the workpiece at any given moment (i.e., $0 \le \theta \le 2\pi d/h$).

The parameters K_s and K_{rt} are dependent on the tool and workpiece material, and power functions of average chip thickness, $\bar{t}_c$ ($= 2f_t/\pi$ in the given experimental condition) [29]. These parameters were obtained by curve-fitting Eq. (1) to the measured cutting-force data. Various experimental conditions were used for data collection (i.e., $f = 45$, 60, 72, and 75 mpm, $d = 0.5$ and 1 mm, $d_r = 8$, 10, and 12 mm, and $N_s = 1200$ and 1500 rpm). Nonlinear regression yields: $K_{rt} = 0.163\bar{t}_c^{-0.353}$ (unitless), and $K_s = 800\bar{t}_c^{-0.197}$ N/mm^2.

The predicted forces agree well with measured data as shown in Fig. 2. The force signal of which frequency is higher than the principal component (i.e., $N_s \cdot M/60$ Hz) are not predicted in the model. The source of the high frequency signal includes tool runout (i.e., cutter-axis offset and tilt) [31], tool deflection, vibration (i.e., due to cutter, machine tool and workpiece dynamics) [32], dynamome-

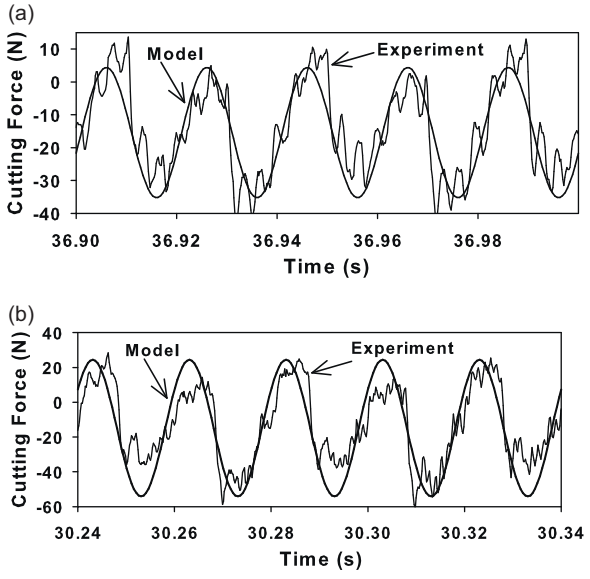

Fig. 2. Comparison of cutting forces (a) F_x and (b) F_y predicted by the mathematical model, and the cutting forces measured with the tool dynamometer. Machining conditions are: feed rate = 60 mpm, spindle speed = 1500 rpm, depth of cut = (a) 0.5 mm, and (b) 1.0 mm.

Table 1
RMS error between the cutting-force model and measured data (F_x) for various cutting conditions (spindle speed = 1500 rpm).

Mill diameter (mm)	Feed rate (mpm)	Depth of cut (mm)	RMS error (N)
8	45	0.5	7.04
8	60	0.5	8.05
8	60	1.0	14.36
8	60	1.5	17.70
8	75	0.5	9.08
10	45	0.5	6.31
10	60	0.5	8.39
10	60	1.0	15.85
10	60	1.5	24.33
10	75	0.5	9.88
12	45	0.5	13.24
12	60	1.0	20.27
12	60	1.5	25.99

ter dynamics [33], and electronics noise [34]. Root-mean-square (RMS) errors between the measured and predicted cutting force (F_x) are calculated for various cutting conditions (Table 1). The spindle speed was fixed at 1500 rpm as the numerical simulation was also run under this condition. When the depth of cut is small (i.e., 0.5 mm), and the model agrees well with the cutting-force data. However, the RMS error increases as the depth of cut grows. This deviation from the model was also observed in the FLC simulation results (Section 5). According to Eq. (1), the cutting force is not a function of the mill diameter. However, the tabulated result indicates that the model error also increases when the mill diameter increases. These observations indicate that model need improvement if more accurate prediction of cutting forces is necessary.

4. Design of fuzzy-logic cutting-force controller

The cutting force is shown to be a sinusoidal function of which amplitude and dc-offset change in response to time-varying cutting conditions. As a result, a linear transfer function is not easily obtained. Therefore, a fuzzy-logic controller (FLC) was designed instead of linear control algorithms.

4.1. Control of cutting forces by adjusting feed rate

In this section, a controller that modifies a cutting parameter (i.e., feed rate) to follow a set point of a desired cutting force F_d, is designed. The representative force for feedback can be average, minimum, maximum, or RMS values sampled over a period. The reason of using such "quasi-static" quantities is that feedbacking dynamic force signal sampled in high frequency makes the overall control system unstable. A cutting forces is a rapidly changing sinusoidal signal. As a result, the control action would strive to follow F_d by adjusting the feed rate in a similar sinusoidal pattern. Therefore, the cutting force is defined as a maximum value of the magnitude of the force vector (i.e., $\sqrt{F_x^2 + F_y^2}$) per spindle rotation for the following reasons: (1) The duration of a single rotation is twice the period of the sinusoidal force signal. Thus, forces acting on all flutes will be accounted for. (2) The feed rate is adjusted in a conservative manner using the "maximum force" as a set point to prevent tool breakage or motor-drive overload. (3) The spindle speed used in this research is less than 4500 rpm, which is equivalent to 17 ms for a rotation. This is enough time for the FLC algorithm to calculate a feed rate command for the next step.

The block diagram in Fig. 3 shows the double-loop structure of the FLC. A inner-loop PD controller adjusts the input of a feed-motor drive to follow the desired feed rate f_d. Sampling rate for the inner loop is 1 ms, and the discrete notation is k. The FLC of the outer loop obtains the maximum cutting force, compares with F_d, and determines an appropriate increase or decrease of the reference feed rate f_{ref} to yield the desired feed rate f_d. Finally, the outer FLC loop delivers f_d to the velocity controller. For k', the sampling step of the FLC, the following relationship holds: $k' = n \cdot k$, where n is the number of sampling steps of the velocity-control loop, which is required to complete a single sampling step of the FLC.

4.2. Servo-controller design

A discrete-domain transfer function (i.e., input voltage $u(k)$ to output position $y(k)$) of y-axis feed system of the CNC vertical machining center is obtained using a frequency-domain system identification, assuming that the model is the second-order system:

$$\frac{y(k)}{u(k)} = G_p(z^{-1}) = \frac{0.00257z^{-1} + 0.00241z^{-2}}{1 - 1.820z^{-1} + 0.820z^{-2}} \quad (2)$$

A PD controller was designed. Firstly, a proportional gain is selected such that a closed-loop-system response to a step input (i.e., $r(k) = 100\ \mu m$) has a fast rise-time. Secondly, a small derivative gain is added so that no overshoot is observed in the step response because the cutting tool should not over-run a desired position in milling processes. The PD controller is a function of tracking error $e(k)$:

$$u(k) = 0.001396e(k) - 0.0001e(k-1). \quad (3)$$

Now an interpolation loop generates a trajectory that $y(k)$ should follow:

$$r(k) = r(k-1) + f_d(k') \cdot T_s, \quad (4)$$

where T_s is the sampling rate of the velocity-control loop.

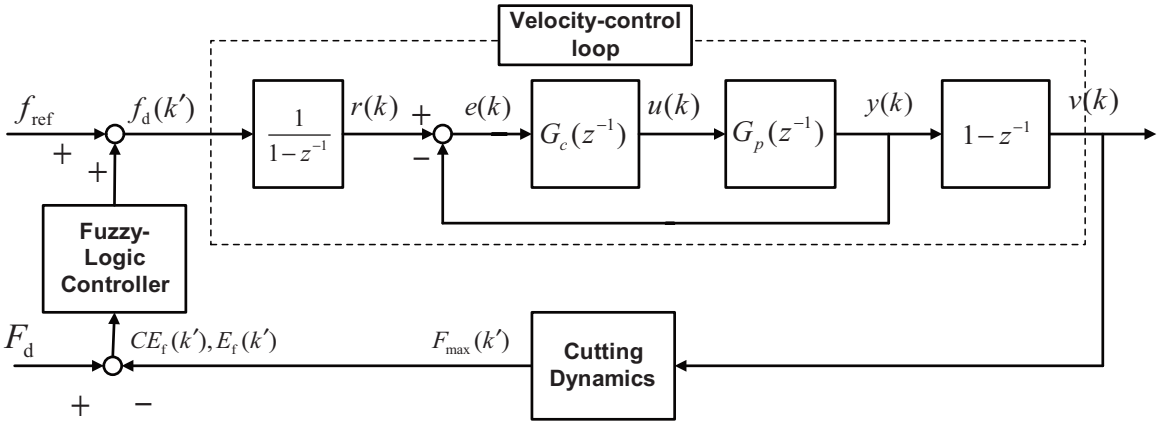

Fig. 3. Block diagram of the fuzzy-logic cutting-force controller.

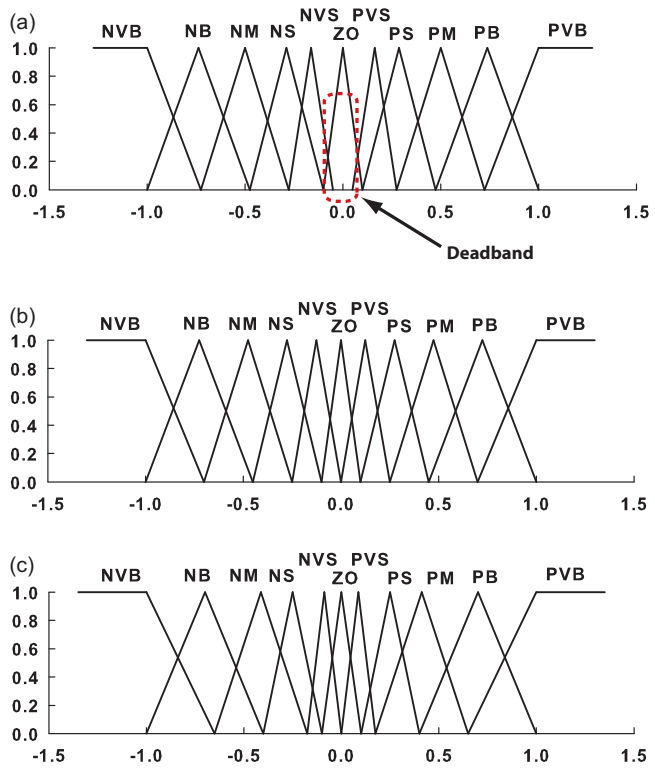

Fig. 4. Membership functions of the fuzzy-logic controller for the input variables (a) $E(k')$ and (b) $CE(k')$, and the output variable (c) $CO(k')$.

4.3. Force-controller design

The difference between the measured cutting force $F_{max}(k')$ and the reference cutting force F_d, is $E(k')$. The value of $E(k')$ and its difference $CE(k')$ are calculated in the FLC loop. The FLC uses membership functions depicted in Fig. 4a and b to translate $E(k')$ and $CE(k')$ into linguistic variables. The input variables are normalized as follows:

$$\bar{E}(k') = \frac{E(k')}{F_d}, \quad \text{and} \quad \overline{CE}(k') = \frac{CE(k')}{F_d}. \tag{5}$$

The linguistic variables of the FLC output are determined by referring the linguistic variable $\bar{E}(k')$ and $\overline{CE}(k')$ to the rule base (Table 2). The FLC output is a feed-rate adjustment for the next force-control step, and is then converted into a real value using the membership function for the controller output $\overline{CO}(k')$ (Fig. 4c). The $\overline{CO}(k')$ is also normalized, and thus the value should be multiplied by a proportional coefficient K_v to yield the real feed-rate command:

$$f_d(k') = f_d(k'-1) + K_v \cdot \overline{CO}(k'). \tag{6}$$

The membership functions (Fig. 4) were obtained by trial and error using numerical simulations, and cutting experiments. The rule base (Table 2) was also determined using the empirical method that Braee and Rutherford [35] suggested, and fine-tuned using the numerical simulation and cutting experiments. As seen in Fig. 4a, the membership function for $E(k')$ has a deadband. The maximum cutting force F_{max} continuously varies due to machine-tool vibration even at a constant feed rate. Without the deadband, the feed-rate command also continues to oscillate even after F_d is reached.

5. Verification of the fuzzy-logic controller with numerical simulation and experiments using a dynamometer

The numerical simulation and experiments for cutting-force control were performed using the FLC designed in the previous section. In this work, only d (depth of cut) is assumed to vary as the workpiece material or spindle speed are usually constant. The Kistler dynamometer was used to measure cutting forces. The spindle axis travels only in the y direction.

5.1. Numerical simulation

The depth-of-cut profile of the workpiece is shown in Fig. 5a. The initial feed rate for air cut was set to be 60 mpm (f_{ref}), and the target cutting force F_d was 160 N. The spindle speed (N_s) was 1500 rpm, and the diameter (d_r) of the two-flute end mill was 10 mm. The mathematical model in Eq. (1) was used to calculate the maximum cutting force per spindle rotation, $F_{max}(k')$.

As seen in Fig. 5b, $F_{max}(k')$ was drastically increased when the depth of cut d stepped from 1.5 to 3.0 mm (t = 2.7 s). The FLC successfully regulated the force at 160 N by lowering the feed rate to 70 mpm. When d became 1.5 mm again (t = 5.3 s), the cutting force also decreased to 100 N. Then the FLC increased the feed rate to 190 mpm so the cutting force was maintained at 160 N.

5.2. Experimental results

The FLC was applied to a model plant (ACE-V30). The control algorithm was implemented using the DSPACE DAQ and DSP systems. The cutting forces were sampled every 1 ms, and the maximum force per spindle rotation was numerically calculated. In addition to the depth-of-cut profile identical to that in the simulation (Case 1), two more workpieces were used in the experiment (Case 2 and 3). The value of d changed four times in Case 2 (Fig. 7a), and linearly increased with the slope of 0.5 in Case 3 (Fig. 8a). The initial feed rate (also for air cut) was 120 mpm, and the feed rate was limited to 240 mpm to prevent potential machine-tool damage.

Case 1. F_d was also 160 N. It should be noted that the nominal feed rate is 0 mpm during air cut (Fig. 6b) because the FLC algorithm starts working as soon as any cutting force is detected. When d was

Table 2
The rule base of the FLC. Linguistic sets are: PVB (positive very big), PB (positive big), PM (positive medium), PS (positive small), PVS (positive very small), ZO (Zero), NVS (negative very small), NS (negative small), NM (negative medium), NB (negative big), and NVB (negative very big).

$\bar{E}/\overline{CE}$	NVB	NB	NM	NS	NVS	ZO	PVS	PS	PM	PB	PVB
NVB	NVB	NVB	NVB	NVB	NVB	NVB	NB	NM	NS	NS	ZO
NB	NVB	NVB	NVB	NB	NM	NM	NM	NS	NS	ZO	PS
NM	NVB	NVB	NB	NM	NM	NS	NS	NS	ZO	PS	PS
NS	NVB	NB	NM	NM	NS	NVS	NVS	ZO	PS	PS	PM
NVS	NVB	NB	NM	NS	NVS	NVS	ZO	PVS	PS	PM	PB
ZO	NB	NM	NS	NVS	NVS	ZO	PVS	PVS	PS	PM	PB
PVS	NB	NM	NS	NVS	ZO	PVS	PVS	PS	PM	PB	PVB
PS	NM	NS	NS	ZO	PVS	PVS	PS	PM	PM	PB	PVB
PM	NS	NS	ZO	PS	PS	PS	PM	PM	PB	PVB	PVB
PB	NS	ZO	PS	PS	PM	PM	PB	PB	PVB	PVB	PVB
PVB	ZO	PS	PS	PM	PB	PVB	PVB	PVB	PVB	PVB	PVB

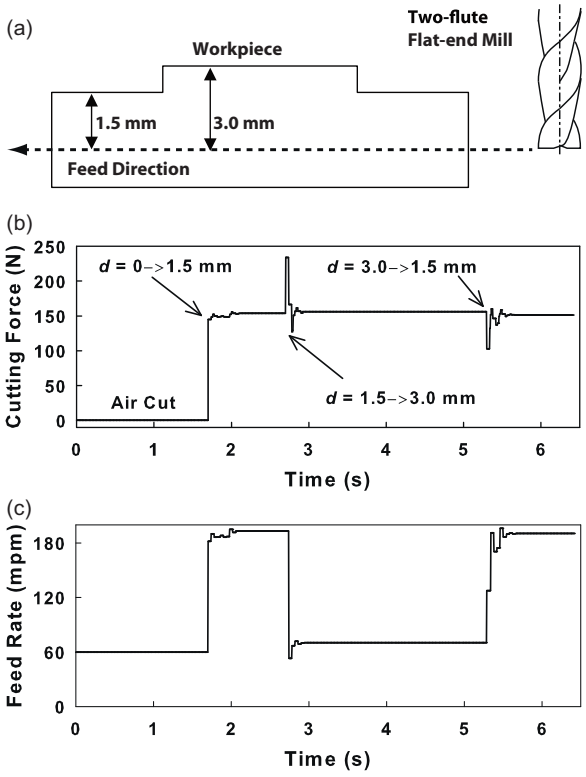

Fig. 5. Simulation result of cutting-force control when the workpiece has (a) the step-wise cutting-depth profile: (b) the maximum cutting force $F_{max}(k')$, and (c) the feed rate $f_d(k')$.

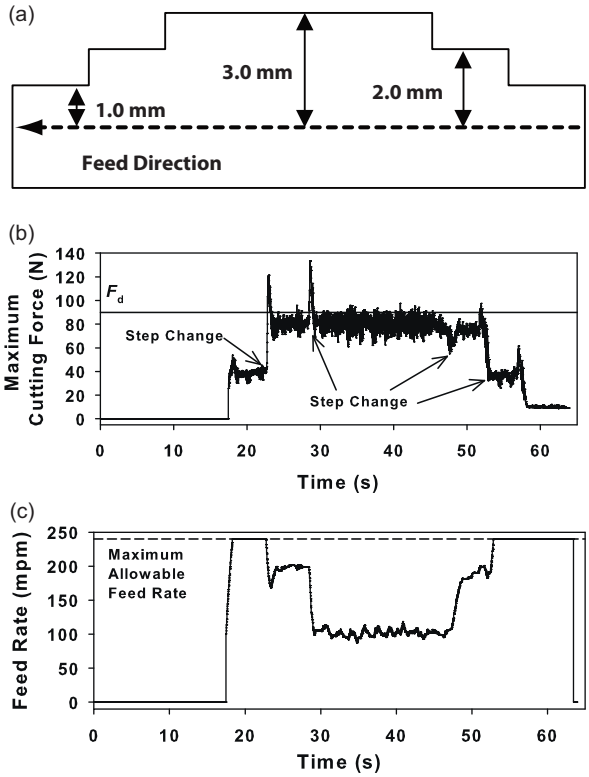

Fig. 7. The experimental result for Case 2: (a) the depth-of-cut profile, (b) the measured maximum cutting force, and (c) the feed-rate command.

only 1.5 mm, $f_d(k')$ was increased to 240 mpm, and F_d was maintained (Fig. 6a). When d was 3 mm, the cutting force overshot to 300 N. Then the FLC maintained F_d by reducing feed rate. This experimental result was similar to the numerical simulation with the only differences being the high-frequency contents of the observed maximum force per spindle revolution (Fig. 6a). Therefore, $f_d(k')$ constantly oscillates accordingly, while the numerical simulation was able to maintain a constant $f_d(k')$ value. The "deadband" (Fig. 4a) prevented unacceptable vibration in the feed command.

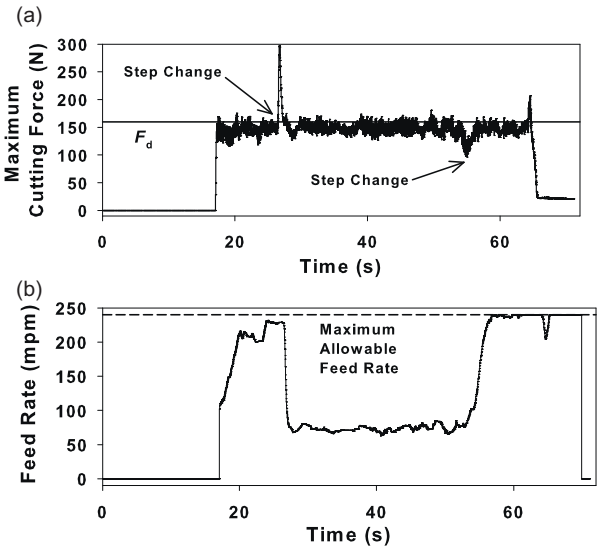

Fig. 6. The experimental result for Case 1: (a) the measured maximum cutting force, and (b) the feed-rate command.

The sudden increase (overshoot) in the cutting force when d increased from 1.5 to 3 mm was larger than the predicted value.

Case 2. F_d was 90 N for Case 2. Fig. 7 also shows similar results to that of Case 1. When d was low (i.e., 1 mm), the desired cutting force of 90 N could not be maintained even after the feed rate was pushed to the upper limit of 240 mpm. However, F_d was well regulated when d was larger (i.e., 2 and 3 mm).

Case 3. The FLC also works well for the case where the cutting depth is continuously increasing (Fig. 8). As for Case 2, if the value of d is too low, the target cutting force 160 N could not be maintained. However, F_d was well maintained by increasing feed rate continuously after this short period of low d.

6. Estimation of cutting force using motor currents

Spindle-motor and feed-motor currents were compared as a practical alternative to the dynamometer. A dc value that represents the current is required to obtain a linear relationship with the quasi-static force. Thus, currents of an ac induction motor (i.e., time-varying polyphase signal) were converted to a dc-equivalent value using RMS conversion: $I_{RMS} = \sqrt{\left(I_U^2 + I_V^2 + I_W^2\right)/3}$, where I_U, I_V, and I_W are U-, V-, and W-phase currents, respectively.

6.1. Feed-motor current as a cutting-force sensor

6.1.1. The equation of motion for a feed system

The output torque of the motor T_m is proportional to the rotor current I. This torque accelerates the equivalent feed-system inertia J_e. In addition, this torque is used to overcome viscous damping B, coulombic friction T_f, and the cutting torque T_c acting on the feed system. The equation of motion can be expressed as [24]:

$$T_m = K_t I = J_e \frac{d\omega}{dt} + B\omega + T_f + T_c, \quad (7)$$

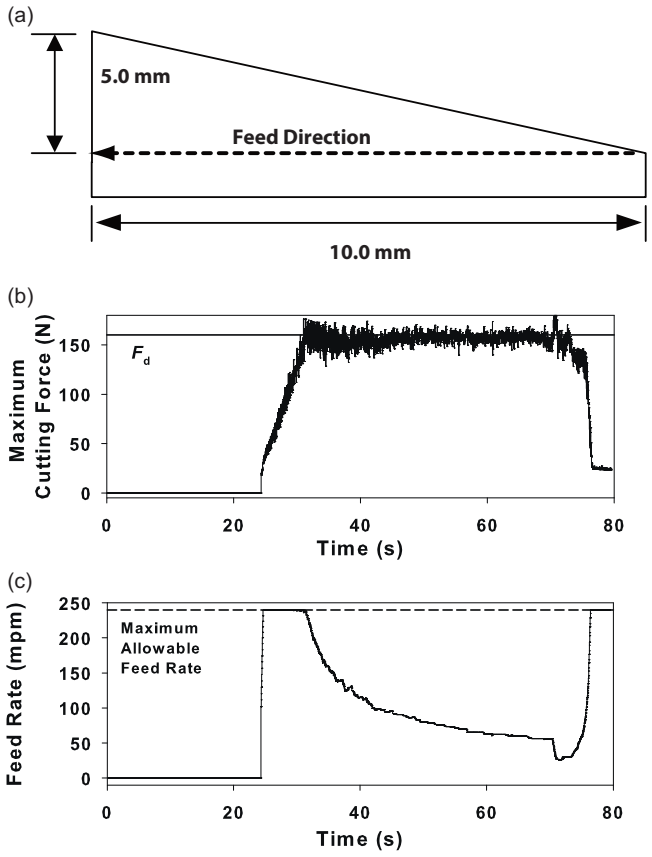

Fig. 8. The experimental result for Case 3: (a) the depth-of-cut profile, (b) the measured maximum cutting force, and (c) the feed-rate command.

where K_t is the torque constant of the motor. The cutting torque is expressed as $T_c = K_f \cdot F_c$, where F_c is the cutting force and K_f is the cutting-force-transmission gain. In this expression, T_f is important for the feed system, where a strong columbic friction exists in the guideway [24].

6.1.2. The friction torque as a function of current

In Eq. (7), the cutting torque T_c is 0 when the tool does not engage a workpiece ($F_c = 0$), and when a feed rate is constant without acceleration or deceleration ($d\omega/dt = 0$). After both sides of the equation are divided by K_t, we have:

$$I(\omega) = \bar{B}\omega + \bar{T}_f \,\mathrm{sgn}(\omega), \tag{8}$$

where $\bar{B} = B/T_t$, and $\bar{T}_f = T_f/K_t$. The columbic friction and viscous damping terms in Eq. (8) were obtained by measuring the motor current I in constant-feed experiments without cutting. The currents were measured using the hall-effect-sensor board made in-house. The bandwidth of each sensor is 10 kHz, which is high enough for current measurement in the cutting process where the tooth-passing frequency is up to 200 Hz (i.e., spindle speed $N_s = 6000$ rpm for a two-flute end mill). The sampling frequency was 1 kHz, and a low pass filter with a cutoff frequency of 200 Hz was used to reduce noise. The feed rate f and angular velocity ω have the following linear relationship for the given feed system: 1 ω rad/s = 95.492 mpm.

Current was measured when the table traveled 0.2 m back and forth in y direction at feed rates of 3–10,000 mpm. The current as a function of ω was obtained by linear regression: $I(\omega) = 1.454 \times 10^{-6}\omega + 1.224$ A (positive direction), and $I(\omega) = 1.380 \times 10^{-6}\omega + 1.145$ A (negative direction), except the low feed-rate range of 286 to 28,648 rad/s ($\simeq$ 3 to 300 mpm). In this range, I is observed to be a convex function of ω (data not shown) [36]. Thus, the frictional torque must be interpolated from the collected data when operating in this low feed-rate regime. It is interesting to note that the tribology depends on the feed direction.

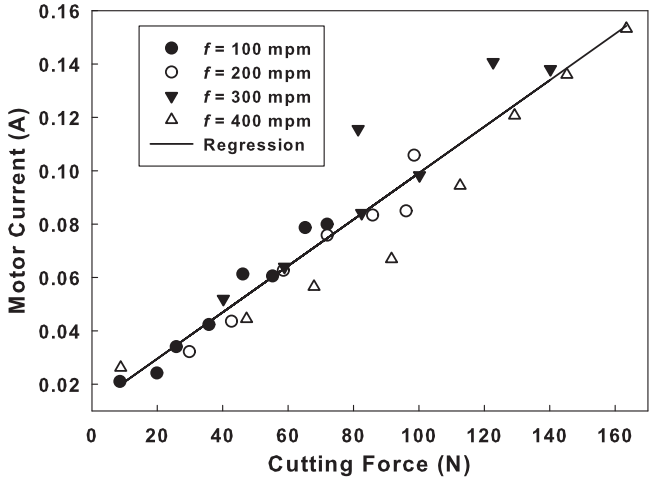

Fig. 9. Relation between cutting average force and RMS current at various cutting conditions. The spindle speed is 3000 rpm.

6.1.3. The RMS current as a function of cutting force

The relation between the motor current and cutting force was also obtained experimentally. The aluminum workpiece was milled with various cutting conditions (i.e., $f = 100$–400 mpm, $d = 0.5$–4 mm). It was observed that K_f for time-varying cutting forces F_c varied for a different feed condition. It may be attributed to the dc term in Eq. (1). However, it is observed that the average cutting force per spindle revolution in y direction $F_{c,y,avg}$ and the resulting current have a rather simple linear relationship. The contribution of viscous damping and the friction was subtracted from the current. This quasi-static relationship is depicted in Fig. 9: $I = 8.7 \times 10^{-4} F_{c,y,avg} + 1.22 \times 10^{-2}$ A. The current increases linearly as the average cutting force increases, and is independent of the feed rate. To account for tribological effects, Eq. (7) can be rewritten as:

$$I = \bar{B}\omega + \bar{T}_f + F_{c,y,avg}\bar{K}_f, \tag{9}$$

where $\bar{K}_f = K_f/K_t$. The linear regression yields ($f > 300$ mpm): I $8.7 \times 10^{-4} F_{c,y,avg} + 1.454 \times 10^{-6}\omega + 1.236$ A (positive direction). However, this quasi-static current-force relation is observed to depend on the spindle speed N_s. Thus, the current-force relation needs to be reevaluated for different N_s values.

It is interesting to note that the dynamic cutting force can be predicted, but in limited cases: (1) the relationships between the current and force in Eq. (1) for both dc and ac terms are known; (2) the tooth-passing frequency is less than 20 Hz. The predicted force is compared to the measured force with a good agreement as seen in Fig. 10. Presently, these two terms are shown to be unique for a given cutting condition. So it may be challenging to obtain the dynamic-force-to-feed-current relationship that can be applied for a wide variety of cutting conditions.

6.1.4. Limitations in using the feed-motor current

Again, the bandwidth of feed-motor current for dynamic cutting-force prediction is less than 20 Hz ($N_s = 600$ rpm). The current signal is distorted at a higher frequency. The low bandwidth is a significant limitation because the tooth-passing frequency commonly goes up to 400 Hz.

The strong frictional torque is also problematic. The frictional torque is a significant fraction of the total disturbance torque, and

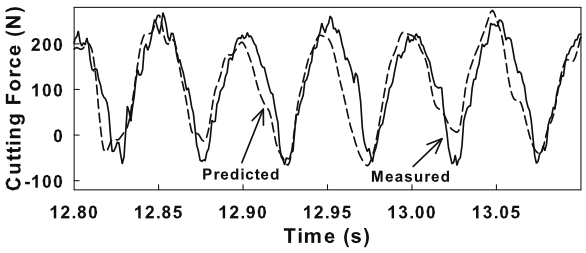

Fig. 10. Comparison of the measured and estimated cutting force of *y*-axis feed system. The cutting condition is: depth of cut = 1.5 mm, feed rate = 150 mpm, spindle speed = 600 rpm.

if the tribology in the guideway changes, this term will also change. Thus, the frictional torque term should be frequently reevaluated.

The model given in Eq. (8) is based on the premise that the feed motion is in steady state. As a result, if the feed rate is modified by the fuzzy-logic controller (FLC), this model is not accurate anymore. Furthermore, a single axis only provides information on the cutting force of that axis. Thus, information on an additional axis is required to have a resultant force F_c. Consequently, the feed system may not be adequate as a force sensor for the FLC.

6.2. Spindle-motor current as a force sensor

Power transmission of the spindle system is very different from that of the feed system. Mechanical power of a drive motor is delivered to a cutting tool through a pulley-belt-gear system. This system results in a low bandwidth of spindle-motor current as a force sensor (<5 Hz), and thus the dynamic force information is highly distorted [22]. Furthermore, the rotational angle should be known in order to calculate *x*- or *y*-directional components from the cutting torque. Due to these limitations, it is not practical to use the spindle motor current to predict dynamic cutting forces as done with feed-motor current (e.g., Fig. 10). Instead, average or maximum cutting force per tool revolution is useful for implementation of the FLC.

6.2.1. The equation of motion for a spindle system

The same mathematical model, Eq. (7), can also be used for the spindle system. Because the spindle is revolving in one direction, the disturbance torque is now expressed as: $T_d = T_f + K_f F_{c,t}$.

6.2.2. The friction torque as a function of current

The tribological effects (i.e., $B\omega + T_f$) were obtained by increasing N_S from 300 to 6000 rpm without cutting. The relation between the spindle speed and the current is depicted in Fig. 11. The current is a nonlinear function of N_S. As a result, the current due to the tribological effects should be expressed as a single term $T_f(\omega)$. This is not an issue since N_S is commonly fixed during milling processes.

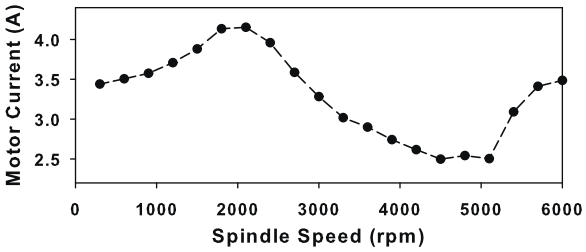

Fig. 11. The RMS current due to tribological effects is measured in air-cut experiments where the spindle speed is increased from 300 to 6000 rpm with an increment of 300 rpm per step.

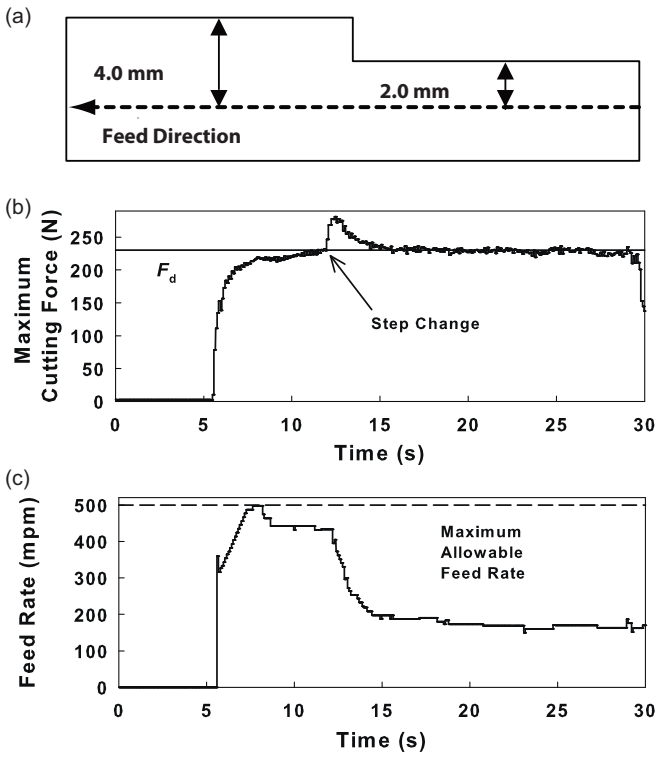

Fig. 12. The experimental result for Case 1: (a) the cutting-depth profile of the workpiece, (b) the maximum cutting force, and (c) the feed-rate command.

6.2.3. The RMS current as a function of cutting force

A cutting experiment similar to the case of the feed-drive system was performed (d = 5–40 mm, N_S = 4500 rpm, f = 150, 300, and 450 mpm). The relationship between average force and current was linear as for the case of the feed system (data not shown). However, the quasi-static sensitivity of the spindle-motor current was much higher than that of the feed-motor current [37]. For the feed system (N_S = 4500 rpm), the *average* feed-motor current per spindle revolution has the slope of 2.128×10^{-4} A/N, but for the spindle system the slopes are an order of magnitude higher at this spindle speed: 6.405×10^{-3} (150 mpm), 7.565×10^{-3} (300 mpm), and 5.451×10^{-3} A/N (450 mpm). Consequently, the spindle system is better than the feed system because it has higher quasi-static sensitivity, and provides resultant force information with a single axis.

The *maximum* cutting force per spindle revolution was also obtained for the FLC with the same experimental condition: $I = 5.762 \times 10^{-3} F_{c,max} + 3.206$ A (150 mpm), $5.981 \times 10^{-3} F_{c,max} + 3.537$ A (300 mpm), and $3.867 \times 10^{-3} F_{c,max} + 3.542$ A (450 mpm). It should be noted that the current-force relation changes as the feed rate changes. Thus, this fact should be accounted for in real time when predicting the maximum cutting force $F_{c,max}$ for the FLC.

7. Experimental results of cutting force control using the fuzzy-logic controller and spindle-motor current

In this section, the spindle motor current and the FLC were used to maintain a constant cutting force on similar workpieces used in Section 5. Three cases for different profiles of the cutting depth were used. For Case 1, the depth of cut d was increased from 2 to 4 mm as seen in Fig. 12a. For Case 2, there were two consecutive steps of d of which step size is higher than the profile in Fig. 5a (i.e., 4–8 mm, and 8–4 mm). For Case 3, d increased continuously, and the slope (0.8) is higher than the profile in Fig. 8a. The initial feed was 120 mpm and the upper limit of feed rate was

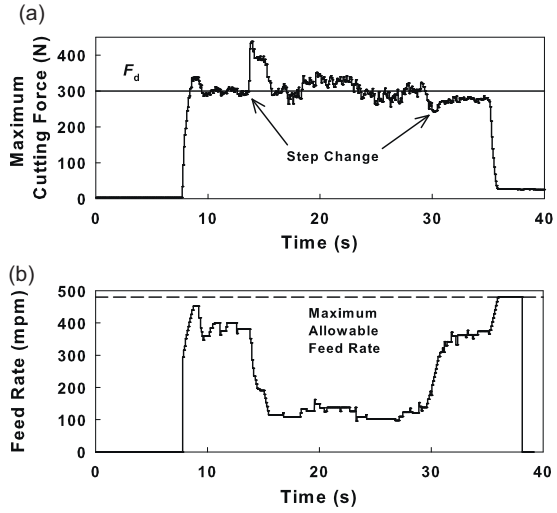

Fig. 13. The experimental result for Case 2: (a) the maximum cutting force, and (b) the feed-rate command.

480 mpm (note: 500 mpm for Case 1). The spindle speed was fixed at 4500 rpm.

As the current-force relation is a function of feed rate, in order to update the cutting force accurately in real time the current-force relation at different feed rates needs to be predetermined as the feed rate continuously changes. Thus, the spindle-motor current, 2.506 A, which was equivalent to the maximum cutting force 230 N, was set as F_d. As seen in Fig. 12b, the FLC successfully maintained the constant cutting forces for Case 1. When the depth of cut d was as large as 8 mm, the output force oscillated around the reference points (300 N for Case 2) as seen in Fig. 13a. A similar result was observed for Case 3, where F_d was 330 N (Fig. 14b). At this magnitude of cutting force, a strong low-frequency oscillation of the estimated maximum cutting force was observed, due to low frequency oscillation of the RMS current. As a result, the maximum cutting force continued to vibrate even though the constant feed rate was maintained. Thus, the control action is also oscillating beyond the deadband in the membership function (Fig. 4a). If we expanded the deadband, a steady-state offset in the cutting force was increased. Therefore, a band-pass filter for the current signal could be used to remove this low-frequency oscillation of the quasi-static current signal.

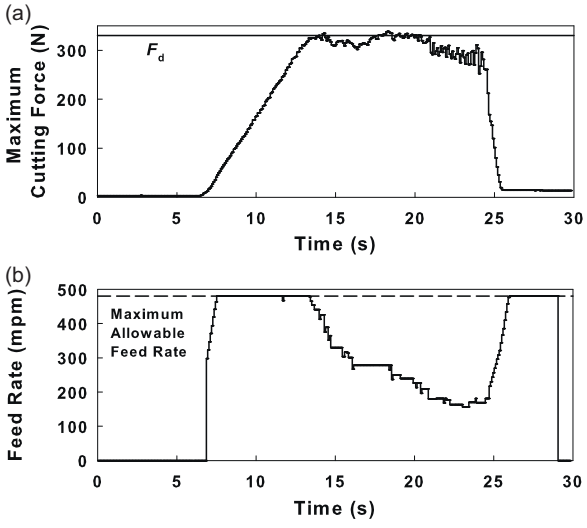

Fig. 14. The experimental result for Case 3: (a) the maximum cutting force, and (b) the feed-rate command.

8. Conclusions

A control system that increases the metal-removal rate, while maintaining a constant cutting force, is presented in this research. The advantages of this control system are: (1) a fuzzy-logic algorithm is simple to design and yet shows a good force-tracking performance, and (2) the control system measures spindle-motor current to sense cutting force instead of using an expensive and impractical tool dynamometer.

The transfer function between cutting force and feed rate is known to be nonlinear and time varying, and thus it is difficult to design a model-based controller, which can effectively cope with persistent variation of cutting dynamics. Because the FLC is based on the knowledge of an experienced human operator, exact information on the transfer function is not required. In this work, the FLC was successful in maintaining a reference cutting force in real time in both numerical simulation, and experiments for two-flute end milling of aluminum workpieces when the tool dynamometer was used.

An important contribution of this work is that motor currents of the feed and spindle system are analyzed and compared in detail as an alternative force sensor that can be used in the proposed control system. It is shown that dynamic cutting forces can be fairly accurately predicted using the feed system under limited conditions. However, both spindle and feed systems have limited bandwidths so that dynamic force can not be estimated accurately at common spindle speeds (e.g., > 4500 rpm). As a result, a quasi-static quantity (i.e., average or maximum force per spindle revolution) for both systems are compared. The spindle system is chosen because it shows higher sensitivity, and the single axis can provide all the necessary information on the resultant force. The spindle speed during milling processes is usually set as a constant. Therefore, parameter variation due to speed change in the spindle system is not an issue unlike in the feed system. As the spindle-current-to-force relation varies with feed rate, this relation could be predetermined within a expected range by extrapolating data sampled at a different feed rate (e.g., every 10 mpm). Such an automated calibration feature could be incorporated in the force controller in the future.

The cutting force was successfully regulated when the FLC was implemented using the spindle-motor current. However, when the depth of cut was large (i.e., $\gg$4 mm), a low-frequency variation of the cutting force was observed even when the feed rate was constant. Therefore, better signal processing (e.g., a band-pass filter that removes both low-frequency variation and high-frequency noise) should be employed to improve steady-state control action of the FLC.

A useful feature could be added to the proposed machining process controller as future work. The difference between the initial feed command and one that makes the spindle current constant is identified as a linear function of wear width of milling cutters when the feed system is in a steady state and the depth of cut does not change [38]. In this way, the tool wear, another important variable in the process control, could be estimated intermittently using the spindle motor current.

References

[1] Ulsoy AG, Koren Y. Control of machining processes. Journal of Dynamic Systems, Measurement, and Control 1993;115(2B):301–8.
[2] Liang SY, Hecker RL, Landers RG. Machining process monitoring and control: the state-of-the-art. Journal of Manufacturing Science and Engineering 2004;126(2):297–310.
[3] Ulsoy AG, Koren Y, Rasmussen F. Principal developments in the adaptive control of machine tools. Journal of Dynamic Systems, Measurement, and Control 1983;105(2):107–12.

[4] Koren Y, Masory O. Adaptive control with process estimation. Annals of the CIRP 1981;30(1):373–6.
[5] Spence A, Altintas Y. CAD assisted adaptive control for milling. Journal of Dynamic Systems, Measurement, and Control 1991;113(3):444–50.
[6] Lauderbaugh LK, Ulsoy AG. Model reference adaptive force control in milling. ASME Journal of Engineering for Industry 1989;111(1):13–21.
[7] Altintas Y. Direct adaptive control of end milling process. International Journal of Machine Tools and Manufacture 1994;34(4):461–72.
[8] Kim T, Kim J. Adaptive cutting force control for a machining center by using indirect cutting force measurements. International Journal of Machine Tools and Manufacture 1996;36(8):925–37.
[9] Charbonnaud P, Carrillo FJ, Ladeveze D. Monitored robust force control of a milling process. Control Engineering Practice 2001;9(10):1047–61.
[10] Huang S, Tan KK, Hong GS, Wong YS. Cutting force control of milling machine. Mechatronics 2007;17(10):533–41.
[11] Kim SI, Landers RG, Ulsoy AG. Robust machining force control with process compensation. Journal of Manufacturing Science and Engineering 2003;125(3):423–30.
[12] Landers RG, Ulsoy AG. Model-based machining force control. Journal of Dynamic Systems, Measurement, and Control 2000;122(3):521–7.
[13] Haber RE, Alique JR, Alique A, Hernández J, Uribe-Etxebarria R. Embedded fuzzy-control system for machining processes results of a case study. Computers in Industry 2003;50(3):353–66.
[14] Zhu JY, Shumsheruddin AA, Bollinger JG. Control of machine tools using the fuzzy control technique. Annals of the CIRP 1982;31(1):347–52.
[15] Kim MK, Cho MW, Kim K. Application of the fuzzy control strategy to adaptive force control of non-minimum phase end milling operations. International Journal of Machine Tools and Manufacture 1994;34(5):677–96.
[16] Tarng YS, Cheng ST. Fuzzy control of feed rate in end milling operations. International Journal of Machine Tools and Manufacture 1993;33(4):643–50.
[17] Haber RE, Alique JR. Fuzzy logic-based torque control system for milling process optimization. IEEE Transactions on Systems, Man, and Cybernetics, Part C: Applications and Reviews 2007;37(5):941–50.
[18] Huang SJ, Shy CY. Fuzzy logic for constant force control of end milling. IEEE Transactions on Industrial Electronics 1999;46(1):169–76.
[19] Prickett PW, Johns C. An overview of approaches to end milling tool monitoring. International Journal of Machine Tools and Manufacture 1999;39(1):105–22.
[20] Shuaib ARN, Garcia-Gardea E, Wu SM. Dynamic analysis of milling machine by torque signal. ASME Journal of Engineering for Industry 1981;103(2):235–40.
[21] Byrne G, Dornfeld D, Inasaki I, Ketteler G, Konig W, Teti R. Tool condition monitoring (TCM)—the status of research and industrial application. Annals of the CIRP 1995;44(2):541–67.
[22] Bertok P, Takata S, Matsushima K, Ootsuka J, Sata T. A system for monitoring the machining operation by referring to a predicted cutting torque pattern. Annals of the CIRP 1983;32(1):439–44.
[23] Stein JL, Wang C. Analysis of power monitoring on AC induction drive systems. Journal of Dynamic Systems, Measurement, and Control 1990;112(2):239–48.
[24] Altintas Y. Prediction of cutting forces and tool breakage in milling form feed drive current measurements. ASME Journal of Engineering for Industry 1992;114(4):386–92.
[25] Stein JL, Colvin D, Clever G, Wang CH. Evaluation of dc servo machine tool feed drives as force sensors. Journal of Dynamic Systems, Measurement, and Control 1986;108(4):279–88.
[26] Lee JM, Choi DK, Kim J, Chu CN. Real-time tool breakage monitoring for NC milling process. CIRP Annals-Manufacturing Technology 1995;44(1):59–62.
[27] Mannan MA, Broms S, Lindustrom B. Monitoring and adaptive control of cutting process by means of motor power and current measurements. Annals of the CIRP 1989;38(1):347–50.
[28] Hashimoto M, Marui E, Kato S. Experimental research on cutting force variation during primary chatter vibration occuring in plain milling operation. International Journal of Machine Tools and Manufacture 1996;36(2):183–201.
[29] Zheng L, Chiou YS, Liang SY. Three dimensional cutting force analysis in end milling. International Journal of Mechanical Sciences 1996;38(3):259–69.
[30] Jain S, Yang DCH. A systematic force analysis of the milling operation. In: The winter annual meeting of the American Society of Mechanical Engineers. 1989. p. 55–63.
[31] Liang SY, Wang JJ. Milling force convolution modeling for identification of cutter axis offset. International Journal of Machine Tools and Manufacture 1994;34(8):1177–90.
[32] Omar O, El-Wardany T, Ng E, Elbestawi MA. An improved cutting force and surface topography prediction model in end milling. International Journal of Machine Tools and Manufacture 2007;47(7–8):1263–75.
[33] Tounsi N, Otho A. Dynamic cutting force measuring. International Journal of Machine Tools and Manufacture 2000;40(8):1157–70.
[34] Kline WA, DeVor RE. The effect of runout on cutting geometry and forces in end milling. International Journal of Machine Tool Design and Research 1983;23(2–3):123–40.
[35] Braae M, Rutherford DA. Selection of parameters for a fuzzy logic controller. Fuzzy Sets and Systems 1979;2(3):185–99.
[36] Kim GD, Choi YJ, Oh YT, Chu CN. Frictional behavior and indirect cutting force measurement in a machining center using feed motor current. Journal of Korean Society of Precision Engineering 1997;14(4):78–87.
[37] Kim GD, Kwon WT, Chu CN. Indirect cutting force measurement and cutting force regulation using spindle motor current. Journal of Korean Society of Precision Engineering 1997;14(10):15–27.
[38] Lee KJ, Lee TM, Yang MY. Tool wear monitoring system for CNC end milling using a hybrid approach to cutting force regulation. International Journal of Advanced Manufacturing Technology 2007;32(1):8–17.